

## Carbon Isotope Fractionation during Diffusion and Biodegradation of Petroleum Hydrocarbons in the Unsaturated Zone: Field Experiment at Værløse Airbase, Denmark, and Modeling

DANIEL B OUCHARD,<sup>†</sup> DANIEL HUNKELER,<sup>\*†</sup> PETROS G AGANIS,<sup>‡</sup> RAMON ARAVENA,<sup>§</sup>  
PATRICK HÖHENER,<sup>||</sup> METTE M. BROHOLM,<sup>⊥</sup> AND PETER KJELDSSEN<sup>⊥</sup>

*Center for Hydrogeology, University of Neuchâtel, Rue Emile Argand 11, 2009 Neuchâtel, Switzerland*

*Department of Environment, University of the Aegean, University Hill, Xenia Building 81100 Mytilene, Greece*

*Department of Earth Sciences, University of Waterloo, 200 University Avenue West, Waterloo, Canada*

*Laboratoire de Chimie et Environnement, Université de Provence, Case 29, 3, Place Victor Hugo, F-13331 Marseille Cedex 3,*

*France Institute of Environment & Resources DTU, Technical University of Denmark, Bygningstorvet B115, DTU, DK-2800 Kgs.*

*Lynghby, Denmark*

A field experiment was conducted in Denmark in order to evaluate the fate of 13 volatile organic compounds (VOCs) that were buried as an artificial fuel source in the unsaturated zone. Compound-specific isotope analysis showed distinct phases in the  $^{13}\text{C}/^{12}\text{C}$  ratio evolution in VOC vapors within 3 m from the source over 114 days. At day 3 and to a lesser extent at day 6, the compounds were depleted in  $^{13}\text{C}$  by up to  $-5.7\%$  with increasing distance from the source compared to the initial source values. This trend can be explained by faster outward diffusion of the molecules with  $^{12}\text{C}$  only compared to molecules with a  $^{13}\text{C}$ . Then, the isotope profile leveled out, and several compounds started to become enriched in  $^{13}\text{C}$  by up to  $9.5\%$  with increasing distance from the source, due to preferential removal of the molecules with  $^{12}\text{C}$  only, through biodegradation. Finally, as the amount of a compound diminished in the source, a  $^{13}\text{C}$  enrichment was also observed close to the source. The magnitude of isotope fractionation tended to be larger the smaller the mass of the molecule was. This study demonstrates that, in the unsaturated zone, carbon isotope ratios of hydrocarbons are affected by gas-phase diffusion in addition to biodegradation, which was confirmed using a numerical model. Gas-phase diffusion led to shifts in  $\delta^{13}\text{C} > 1\%$  during the initial days after the spill, and again during the final stages of source volatilization after  $> 75\%$  of a compound had been removed. In between, diffusion has less of an effect, and thus isotope data can be used as an indicator for hydrocarbon biodegradation.

### Introduction

Natural attenuation is a widely accepted strategy to manage petroleum-hydrocarbon-contaminated sites. The strategy relies on the capacity of indigenous microorganisms to eliminate contaminants from the subsurface under natural conditions and thus tries to limit the use of engineering technologies. To make this strategy reliable, it is important to demonstrate that biodegradation of hydrocarbons is actually occurring at the site. Compound-specific isotope analysis (CSIA) is increasingly used to demonstrate biodegradation in the saturated zone (1–3). The method relies on the occurrence of different degradation rates for molecules with light and heavy isotopes, respectively. The presence of a  $^{13}\text{C}$  atom in the bond that is broken in the initial enzymatic

transformation step can slightly slow down the biodegradation rate, and as a consequence,  $^{13}\text{C}$  compounds accumulate in the remaining contaminant pool over time. While CSIA is increasingly used in groundwater studies, there is little information on its use in the unsaturated zone.

Volatile organic compounds (VOCs) volatilizing from nonaqueous phase liquids (NAPLs) trapped in the unsaturated zone will migrate mainly due to diffusion and create a vapor-phase contaminant plume (4–7) that can affect groundwater quality (8, 9). The vapor-phase transport is influenced by the partitioning of VOCs between gas, water, and solid phases as well as by the geometry of the pore space. In addition to diffusion, density and pressure gradients can contribute to plume expansion (6, 10), whereas biodegradation restricts contaminant spreading. Biodegradation is frequently demonstrated by monitoring the depletion of both molecular oxygen ( $\text{O}_2$ ) and VOC concentrations and the increase of carbon dioxide ( $\text{CO}_2$ ) concentrations in the soil gas (11–14). However, these measurements do not provide clear evidence for the degradation of a specific compound within a mixture. Alternatively, biodegradation can be assessed by fitting a mathematical model to concentration data of controlled field experiments (15) or field sites (16–20). So far, isotope analysis to demonstrate biodegradation in the unsaturated zone mainly focused on the  $\delta^{13}\text{C}$  of soil gas  $\text{CO}_2$  (21–24). However,  $\delta^{13}\text{C}$  variations in  $\text{CO}_2$  can also be due to soil organic matter degradation, and sometimes  $^{14}\text{C}$  measurements were used to distinguish between  $\text{CO}_2$  from recent soil organic matter and from fossil petroleum (25). Only a few studies investigated changes of the isotope ratio of individual VOCs (26, 27). A significant  $^{13}\text{C}$  enrichment in the remaining TCE and DCE in the air phase with respect to the original isotopic signature of PCE was observed by Kirtland et al. (26), while Stehmeier and co-workers (27) monitored  $^{13}\text{C}$  enrichment for an undetermined contaminant.

The aim of this study was to evaluate whether CSIA can be used to demonstrate biodegradation in the unsaturated zone and to evaluate the factors that control the isotope ratios of VOCs. For this purpose, temporal and spatial variations of carbon isotope ratios of a number of VOCs and  $\text{CO}_2$  were measured during a controlled field experiment at the Værløse Airbase, in Denmark. The experimental setup consisted in burying a multicomponent hydrocarbon source in the unsaturated zone of a highly instrumented field site.

\* Corresponding author phone: +41 32 718 2560; fax: +41 32 718 26 03; e-mail: Daniel.hunkeler@unine.ch.

<sup>†</sup> University of Neuchâtel.

<sup>‡</sup> University of the Aegean.

<sup>§</sup> University of Waterloo.

<sup>||</sup> Université de Provence.

<sup>⊥</sup> Technical University of Denmark.

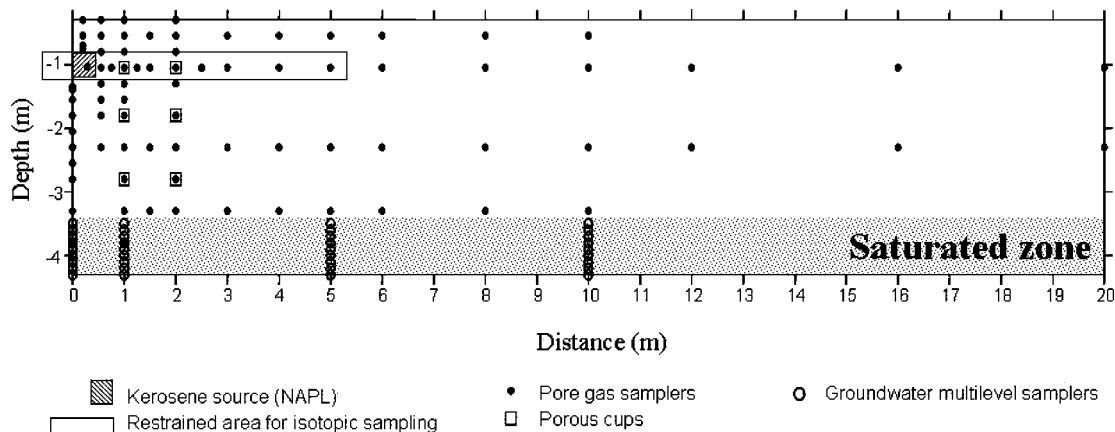


**FIGURE 1.** Cross-section of the field sampling network at the Værløse Airbase experimental site with location of pore gas samplers and porous cups. The area for isotope sampling is delineated by a rectangle. Modified from ref 14.

In the unsaturated zone, isotope ratios can potentially also be affected by diffusion in addition to biodegradation, as indicated by studies on isotope ratios of  $\text{CO}_2$  (28) and  $\text{CH}_4$  (29–32). To gain more detailed insight into the factors controlling the isotope shifts, a numerical model was used that incorporates isotope fractionation, and attempts were made to reproduce the isotope variations observed at the field scale.

## Materials and Methods

**Field Experiment.** A controlled field experiment was realized in a sandy unsaturated zone at the Værløse Airbase, Denmark, as part of the Groundwater Risk Assessment at Contaminated Sites project to simulate a light NAPL spill in the unsaturated zone (5). An artificial NAPL phase was elaborated with a limited number of compounds (Table S1, Supporting Information) to simplify analytical procedures. A total of 10.2 L of the NAPL was mixed with sand, leading to a NAPL saturation of 14.3% of the pore volume. The mixture was then placed at a depth between 0.8 and 1.3 m in a hole with a 0.7 m diameter (5). NAPL persisted throughout the experiment with an estimated saturation of 1.8% after 352 days (33). The evolution of the vapor-phase concentrations at the source followed, in general, Raoult's laws using UNIFAC-derived activity coefficients, except for the less volatile compounds (33). Hence, it can be assumed that for most compounds equilibrium between NAPL and the gaseous phase prevailed at the source.

A dense network of sampling devices was installed in both saturated and unsaturated zones to study the behavior of the VOCs in the system (5). Samples for carbon isotope analyses were taken within a subsection of the experimental area (Figure 1). The selected sampling points were located at 1 m below ground and at a lateral distance of up to 5 m from the center of the source. Soil gas samples were taken with a syringe after purging the soil gas probe. The glass sample bottles were flushed several times via a needle that was introduced through a Mininert valve. During flushing, the Mininert valve was partly unscrewed. In the laboratory, gaseous organic compounds were extracted using solid-phase microextraction as described in Hunkeler and Aravena (34) and analyzed using an Agilent gas chromatograph (GC) connected via a combustion interface to a Micromass Isochrom isotope-ratio mass spectrometer (IRMS) (Micromass, Manchester, U.K.). Initial isotope ratios at the source were determined by the complete evaporation of a small source sample in a 250 mL glass bottle followed by the injection of gaseous samples into the GC-IRMS system via a sample loop. Given that an artificial gasoline mixture was used with relatively few compounds, baseline separation of

all compounds was achieved. Isotope ratios obtained with GC-IRMS are reported using  $\delta^{13}\text{C}$  notation relative to the VPDB standard according to (35):

$$\delta^{13}\text{C} = \left( \frac{R_{\text{sample}}}{R_{\text{reference}}} - 1 \right) 1000 \quad (1)$$

where  $R_{\text{sample}}$  and  $R_{\text{reference}}$  are the ratios  $^{13}\text{C}$  to  $^{12}\text{C}$  of the sample and  $^{13}\text{C}$  to the VPDB reference material, respectively. The standard deviation for reference compounds ( $n = 5$ ) varied between 0.23 ‰ for methylcyclohexane and 0.53 ‰ for 1,2,4-trimethylbenzene with an average of 0.3 ‰.

**Model Simulation.** Simulations were performed using the two-dimensional finite element code MOFAT (36), which was modified in order to deal with the seasonal temperature variation at the field site (20). The numerical model had previously been validated and used to simulate VOC transport in the field experiment conducted at the Værløse Airbase (20) and to estimate biodegradation rates of six selected VOCs. The chosen modeling approach incorporated gaseous transport using Fick's law; equilibrium partitioning between the gas, water, and organic phases; and first-order biodegradation. The isotope evolution was simulated by treating the molecules with a different isotopic composition as separate compounds, here denoted as subspecies, and by attributing to each subspecies a different degradation rate, diffusion coefficient, and initial mass, as outlined in detail in the Supporting Information. Two approaches were used: a two-subspecies approach, which distinguishes between molecules with and without a  $^{13}\text{C}$ , and a three-subspecies approach, which further subdivides the molecules with a  $^{13}\text{C}$  into those with a  $^{13}\text{C}$  at the reactive position and those with a  $^{13}\text{C}$  elsewhere. Previous laboratory studies (37) showed that isotope fractionation during volatilization of BTEX compounds is small (0.17–0.2 ‰). Therefore, the vapor pressure at the source was assumed to be identical for molecules with and without  $^{13}\text{C}$  and to follow Raoult's law. In other words, it was assumed that volatilization is not associated with isotope fractionation. Since the numerical code can only handle a maximum of 5 compounds, that is, only a fraction of the organic species making up the simulated VOC, the remaining mixture compounds were organized into effective pseudo species as described in Gaganis et al. (38).

## Field Results and Discussion

**VOC Concentrations.** The temporal and spatial variations of VOC concentrations at 1 m below the ground surface are illustrated in Figure 2 for selected compounds. The behavior

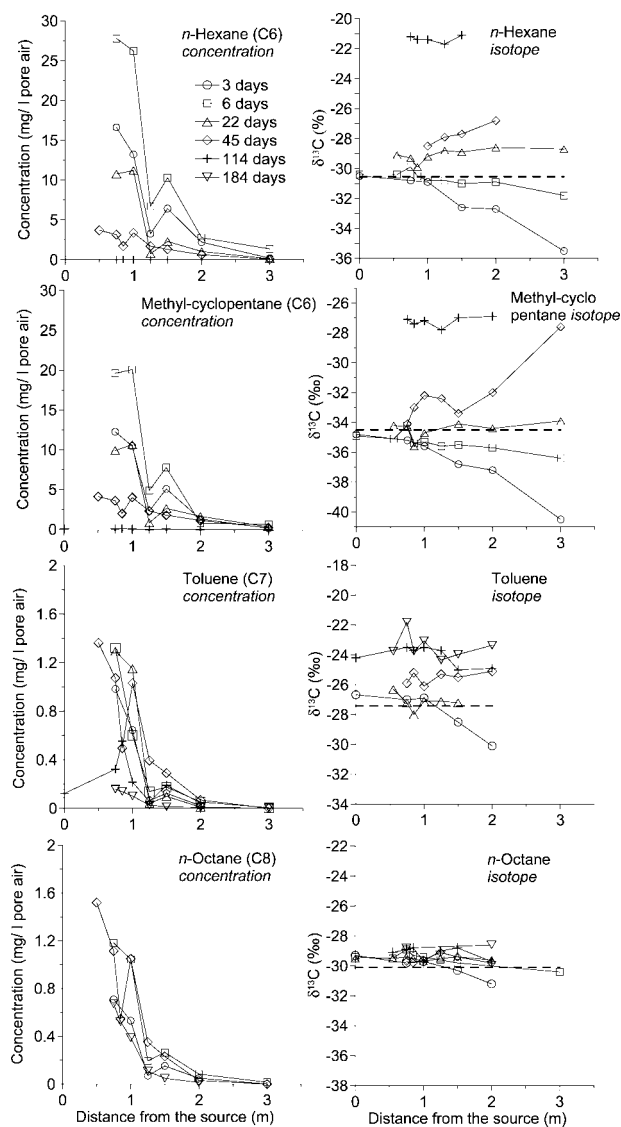


**FIGURE 2. Concentration and  $\delta^{13}\text{C}$  evolution of selected VOCs in the unsaturated zone. The size of the symbols for  $\delta^{13}\text{C}$  corresponds to the uncertainty of the measurement ( $\sigma$ ). The dashed line illustrates the initial  $\delta^{13}\text{C}$  of the source. For additional compounds, see Figure S2, Supporting Information. Measurements were made at a constant depth (1 m) along the main radial monitoring transect.**

of the other compounds is summarized in Table 1 and illustrated in the Supporting Information (Figure S1). In general, the concentrations were high in the source vicinity and decreased with distance from it. After source burial, the compounds migrated outward quickly to a  $>3$  m lateral distance within less than 6 days. For *n*-hexane and methyl-cyclopentane (MCP), the highest concentrations were observed after 6 days, followed by a rapid decrease of the concentrations until day 114, when concentrations dropped below the detection limit. The high initial concentrations, rapid concentration variations, and rapid depletion of these compounds can be explained by their high vapor pressure. For less volatile compounds, such as *n*-octane (Figure 2), the concentrations varied less rapidly, and the compounds persisted longer.

**VOC  $\delta^{13}\text{C}$  Values.** At day 3, all compounds became depleted in  $^{13}\text{C}$  with increasing distance from the source compared to the initial source values (Figure 2 and Figure S1, Supporting Information). The maximal shifts in  $\delta^{13}\text{C}$  ranged from  $-1.9\text{‰}$  for *m*-xylene and *n*-octane to  $-5.7\text{‰}$  for MCP (Table 1). At day 6 or 22, the  $\delta^{13}\text{C}$  of all compounds had

leveled off at the initial value of the source. Afterward, most compounds became enriched in  $^{13}\text{C}$  compared to the initial source value, at first at the fringe of the vapor plume and later also closer to the source (Figure 2).

The initial  $^{13}\text{C}$  depletion with distance was likely due to the faster diffusion of molecules containing only  $^{12}\text{C}$  compared to molecules with one  $^{13}\text{C}$ , leading to a depletion of  $^{13}\text{C}$  at the plume fringe. The largest negative shifts were observed for C6 compounds as the presence of a  $^{13}\text{C}$  atom leads to larger differences in diffusion coefficients for smaller molecules (Table 1). Isotope fractionation due to diffusion was previously observed at the field scale (28) for  $\text{CO}_2$  or postulated on the basis of theoretical investigations (39, 40). Similarly, isotope fractionation during the diffusion of methane was also reported in several other studies (30–32, 41).

The later trend of gradual enrichment in  $^{13}\text{C}$  with distance strongly indicates biodegradation during outward transport of the compounds and corresponds to the pattern typically observed in studies in the saturated zone. Generally, larger shifts were observed for compounds with a larger isotope enrichment factor (Table 1). The final strong  $^{13}\text{C}$  enrichment close to the source and throughout the profile for *n*-hexane and MCP coincided with low concentrations throughout the profile (Figure 2). Sampling of the source at day 113 revealed that *n*-hexane and MCP were no longer detectable in the NAPL mixture (33). Hence, as the amount of compound diminished, isotope fractionation became magnified, as commonly observed in isotope studies and denoted as a reservoir effect. The strong enrichment in  $^{13}\text{C}$  was likely due to preferential biodegradation of light molecules and faster outward diffusion of light molecules, as will be discussed in more detail in the modeling section below.

**Concentration and  $\delta^{13}\text{C}$  of  $\text{CO}_2$ .**  $\text{CO}_2$  concentrations initially ranged between 0.2% and 0.8% and slightly increased to between 0.4% and 0.8% at day 22 and between 1.2% and 2% at day 87. Between days 3 and 114, the  $\text{CO}_2$  became increasingly depleted in  $^{13}\text{C}$  (Figure 3). The depletion of  $^{13}\text{C}$  in  $\text{CO}_2$  confirms that a biodegradation of VOCs occurred. Biodegradation of the VOC is expected to add  $\text{CO}_2$  with a  $\delta^{13}\text{C}$  value  $< -28.2\text{‰}$ , the average  $\delta^{13}\text{C}$  of the nine most degradable VOCs (excluding benzene, cyclopentane, decane, and dodecane). The  $\text{CO}_2$  was generally more depleted in  $^{13}\text{C}$  closer to the source than further away. This trend is likely due to a stronger production of  $^{13}\text{C}$ -depleted  $\text{CO}_2$  close to the source where hydrocarbons were present at higher concentrations.

## Modeling Results and Discussion

Numerical modeling was used to gain additional insight into the contribution of diffusion and biodegradation to the observed isotope evolution. Three different scenarios were simulated: (i) only biodegradation fractionates, (ii) only diffusion fractionates, and (iii) both processes fractionate. *n*-Hexane and *n*-octane were modeled with the two- and three-subspecies approach, toluene and MCP using only the two-subspecies approach (see the Materials and Methods section and Supporting Information). As the two- and three-subspecies approach gave similar results (Table S4, Supporting Information), only the results obtained by one calculation method are presented (Figure 4).

**Isotope Fractionation by Biodegradation.** Figure 4a illustrates the expected  $\delta^{13}\text{C}$  values of *n*-hexane if only biodegradation is associated with isotope fractionation. The *n*-hexane becomes increasingly enriched in  $^{13}\text{C}$  with distance from the source due to preferential degradation of molecules with light isotopes during outward transport. With increasing time, the whole isotope profile tends to shift upward compared to the initial source value. The latter tendency can be explained by a reservoir effect. As the amount of

**TABLE 1. Shifts in  $\delta^{13}\text{C}$ , Difference in Diffusion Coefficients Due To the Presence of a  $^{13}\text{C}$  Atom in the Molecule, Isotope Enrichment Factor Obtained in Separate Microcosm Experiments, and Half-Life for Compound Depletion in Source for Different VOCs**

	maximal $\delta^{13}\text{C}$ shift at day 3 ‰	maximal $\delta^{13}\text{C}$ shift at day 45 ‰	maximal $\delta^{13}\text{C}$ shift at day 114 ‰	$(D_L^d/D_H^e - 1)$ *1000 ‰	carbon isotope enrichment factor for biodegradation ‰	source half-life <sup>a</sup> (days)
<i>n</i> -hexane	-5.0	3.7	9.4	1.5	$-2.2^b \pm 0.4$	14.2
3-MP	-4.1	4.9	9.5	1.5	$-1.1^c \pm 0.1$	11.0
MCP	-5.7	7.2	7.9	1.5	$-1.5^c \pm 0.1$	13.7
MCH	-3.8	1.5	2.6	1.2	$-1.1^c \pm 0.1$	38.9
toluene	-3.4	1.6	3.2	1.3	$-0.7^c \pm 0.1$	66.6
isooctane	-3.0	4.0	3.0	0.9	nd	36.9
<i>n</i> -octane	-1.9	0.2	0.5	0.9	$-0.7^b \pm 0.2$	104.7
<i>m</i> -xylene	-1.9	0.9	1.5	1.0	$-0.8^b \pm 0.1$	161.7
1,2,4-TMB	-2.1	-0.1	0.1	0.8	nd	313.3

<sup>a</sup> Estimated on the basis of measured source composition data from ref 33. <sup>b</sup> From ref 43. <sup>c</sup> From ref 44. nd: not determined. <sup>d</sup>  $D_L$  diffusion coefficient for molecules with  $^{12}\text{C}$  only. <sup>e</sup>  $D_H$  diffusion coefficient for molecules with a  $^{13}\text{C}$ .

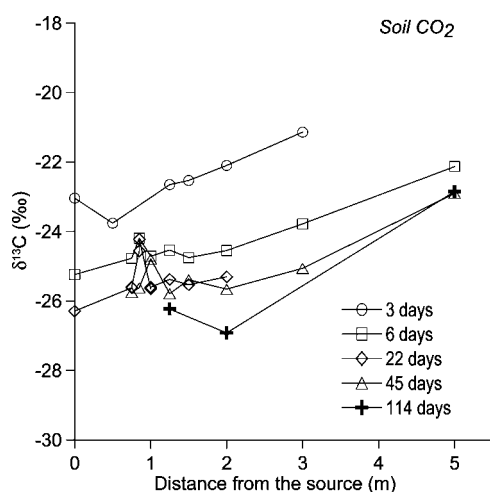


**FIGURE 3. Temporal and spatial variation of  $\delta^{13}\text{C}$  of  $\text{CO}_2$ .**

*n*-hexane at the source diminishes, the continuous preferential removal of molecules with  $^{12}\text{C}$  only by biodegradation becomes noticeable at the source. At day 45, there is relatively good agreement between the general shape of the simulated (Figure 4a) and measured (Figure 2) isotope profiles. However, the calculations fail to reproduce trends observed during day 3 (shift to more negative  $\delta^{13}\text{C}$  values) and later periods (shift to more positive  $\delta^{13}\text{C}$  values close to the source), indicating that during these two phases other processes strongly influence isotope ratios as well.

**Isotope Fractionation by Diffusion.** Figure 4b illustrates the expected  $\delta^{13}\text{C}$  values of *n*-hexane for isotope fractionation by diffusion only. Unlike for biodegradation, *n*-hexane becomes depleted in  $^{13}\text{C}$  toward the fringe of the plume. Similarly as for biodegradation, the whole profile shifts upward with time. This is again due to a reservoir effect. Hence, diffusion has two effects that are both related to the faster diffusion of compounds with  $^{12}\text{C}$  only: the plume fringe is initially depleted in  $^{13}\text{C}$ , and the source becomes enriched in  $^{13}\text{C}$  as the quantity of *n*-hexane remaining diminishes. There is good agreement between simulated (Figure 4b) and measured (Figure 2) isotope profiles for days 3 and 6, confirming that diffusion controls the carbon isotope ratios for  $t < 6$  days.

**Isotope Fractionation by Biodegradation and Diffusion.** Figure 4c shows the modeling results if both biodegradation and diffusion fractionate for *n*-hexane (Figure 4c), as well as for *n*-octane (Figure 4d), toluene (Figure 4e), and MCP (Figure 4f). Isotope measurements from the field experiment are also presented in the same figure. In these modeling simulations,

biodegradation rate coefficients were kept close to mean values reported for the Værlose site, and isotope enrichment factors were manually varied within their range of uncertainty, until the best fit between modeled and measured results was obtained. The values yielding the best fit can be found in Table S3 of the Supporting Information. In general, the model reproduces the measured data well. The average divergence between field measurements and predicted values of  $\delta^{13}\text{C}$  for *n*-hexane and toluene is 0.55‰ and 0.53‰, respectively (Table S5, Supporting Information). The good agreement between measured and simulated values confirms the conceptual model underlying the mathematical simulation, which incorporates isotope fractionation due to diffusion and biodegradation while assuming that volatilization is not associated with isotope fractionation. It also suggests that laboratory-derived isotope enrichment factors from unsaturated batch studies are representative for field conditions.

The model successfully reproduces the different phases of the isotope evolution. In particular, it also reproduces the  $^{13}\text{C}$  enrichment along the entire profile observed at day 114. The calculations suggest that, during this phase, both biodegradation and diffusion contributed to a significant enrichment of  $^{13}\text{C}$  close to the source for *n*-hexane, toluene, and MCP. As indicated by the model, biodegradation (Figure 4a) and diffusion (Figure 4b) alone each led to a shift of about 5‰ close to the source after 114 days for *n*-hexane, while the observed shift (Figure 4c) was twice as large. For *n*-octane, only a small shift was observed close to the source (Figure 4d). This can be explained by the smaller differences in diffusion coefficients for the different subspecies and because less mass is volatilized due to the smaller vapor pressure. As illustrated in Table S2 of the Supporting Information, at least 75% of a compound needs to be removed from the source before a shift in the source isotope ratio of  $> 1$ ‰ occurs.

**Application of CSIA in Unsaturated Zone Studies.** The main potential applications of CSIA include the assessment of biodegradation and the fingerprinting of different petroleum hydrocarbon vapor sources. For both applications, it has to be taken into account that isotope ratios in the unsaturated zone can vary due to diffusion in addition to biodegradation. Diffusion affects the carbon isotope ratio during an initial phase after a spill. The simulation of different scenarios (point source and floating pool) suggested that this phase unlikely lasts for more than 20 days and hence will typically not be sampled at real spills (42). A previous study postulated that a vanishing hydrocarbon source should become depleted in  $^{13}\text{C}$  due to a small inverse isotope effect during volatilization (37). However, this study demonstrates that, to the contrary, the source becomes enriched in  $^{13}\text{C}$

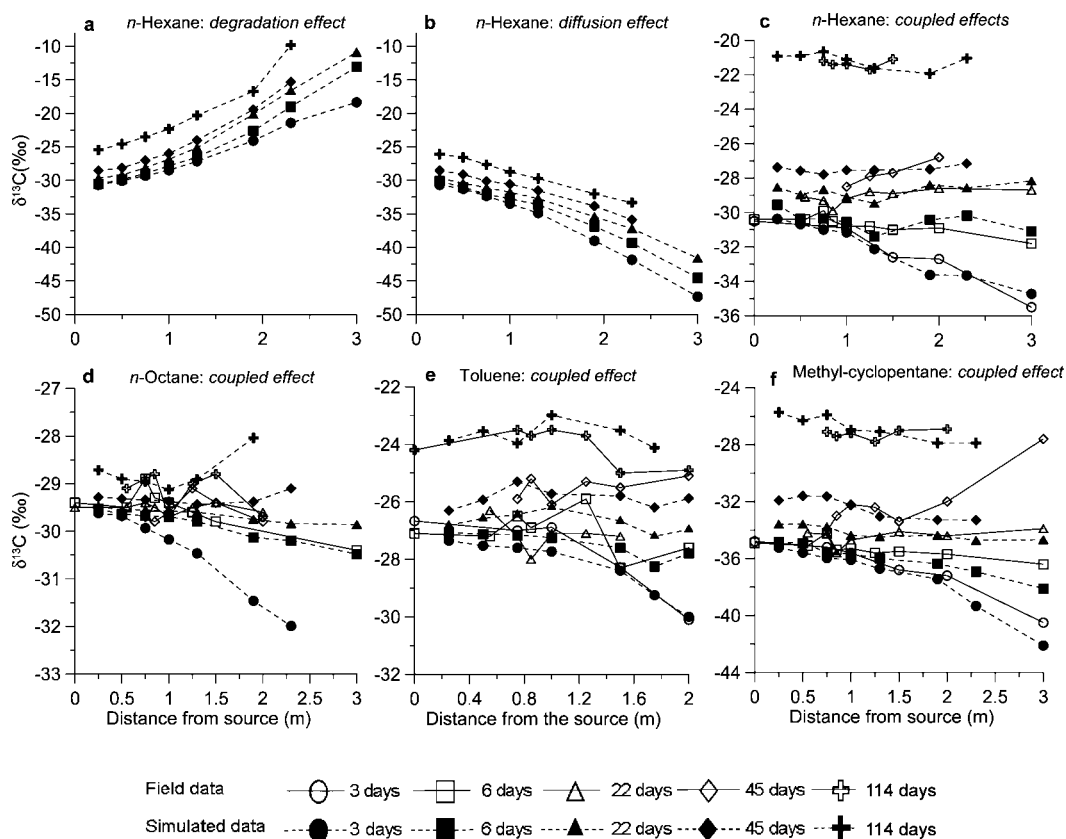


**FIGURE 4.** Simulated  $\delta^{13}\text{C}$  (filled symbols) when only degradation (a) or only diffusion (b) contribute to the isotope fractionation of *n*-hexane. Simulated (filled symbols) and measured (open symbols)  $\delta^{13}\text{C}$  when both processes contribute to isotope fractionation for *n*-hexane (c), *n*-octane (d), toluene (e), and MCP (f). Except for hexane (three subspecies), the two subspecies approach was used.

even in the absence of biodegradation since the mass loss is controlled by diffusion across the porous media. A significant shift of the source isotope ratio ( $>1\text{‰}$ ) due to compound depletion in the NAPL was only observed after  $>75\%$  of the compound was depleted. This shift may help to demonstrate mass removal of a compound from the source. Before this point is reached, the source isotope ratio is expected to be stable, and isotope ratios of the vapor plume can be used as a qualitative indicator for biodegradation, especially for molecules  $\leq \text{C}_8$ . However, since transport occurs by diffusion, the Rayleigh equation cannot be applied to quantify biodegradation. Isotope ratios of larger molecules are less affected by biodegradation and diffusion, and hence their isotope ratio may be used for fingerprinting different vapor sources, for example, in vapor intrusion studies. For larger molecules, hydrogen isotopes are expected to be a more sensitive indicator for biodegradation because isotope enrichment factors for biodegradation are expected to be larger while the effect on diffusion is the same (addition of mass of 1 to the molecule). In summary, this study demonstrates that detailed insight into processes controlling isotope ratios in the unsaturated zone can be gained by combining controlled high-resolution field experiments with numerical modeling. It also demonstrates that CSIA is likely a useful tool for the assessment of biodegradation and fingerprinting of vapor sources. While the occurrence of a diffusion isotope effect can complicate data interpretation, it potentially provides information about mass removal of a compound from a NAPL source.

### Acknowledgments

The project was partly financed by the EU (Fifth Framework Program) and was part of the European project *Groundwater risk assessment at contaminated sites GRACOS*, EVK1-CT-

1999-00029. We also acknowledge financial support provided by the Swiss Federal Office for Education and Research in the frame of COST Action 629 and by the National Science and Engineering Research Council of Canada. The manuscripts benefited from helpful comments of three anonymous reviewers.

### Supporting Information Available

Concentration and isotope data of additional VOCs. Information about the source composition, the source evolution, and the numerical modeling including sensitivity analyses. This material is available free of charge via the Internet at <http://pubs.acs.org>.

### Literature Cited

- (1) Meckenstock, R. U.; Morasch, B.; Griebler, C.; Richnow, H. H. Stable isotope fractionation analysis as a tool to monitor biodegradation in contaminated aquifers. *J. Contam. Hydrol.* **2004**, *75*, 215–255.
- (2) Schmidt, T. C.; Zwank, L.; Elsner, M.; Berg, M.; Meckenstock, R. U.; Haderlein, S. B. Compound-specific stable isotope analysis of organic contaminants in natural environments: a critical review of the state of the art, prospects, and future challenges. *Anal. Bioanal. Chem.* **2004**, *378*, 283–300.
- (3) Elsner, M.; Zwank, L.; Hunkeler, D.; Schwarzenbach, R. P. A new concept to link observed stable isotope fractionation to degradation pathways of organic groundwater contaminants. *Environ. Sci. Technol.* **2005**, *39*, 6896–6916.
- (4) Jury, W. A.; Spencer, W. F.; Farmer, W. J. Behavior assessment model for trace organics in soil: I. Model description. *J. Environ. Qual.* **1983**, *12*, 558–563.
- (5) Christophersen, M.; Broholm, M. M.; Mosbæk, H.; Karapanagioti, H. K.; Burganos, V. N.; Kjeldsen, P. Transport of hydrocarbons from an emplaced fuel source experiment in the vadose zone at Airbase Værlose, Denmark. *J. Contam. Hydrol.* **2005**, *81*, 1–33.

- (6) Conant, B. H.; Gillham, R. W.; Mendoza, C. A. Vapor transport of trichloroethylene in the unsaturated zone: Field and numerical modeling investigations. *Water Resour. Res.* **1996**, *32*, 9–22.
- (7) Silka, L. R. Simulation of vapor transport through the unsaturated zone - interpretation of soil-gas surveys. *Groundwater Monit. Rev.* **1988**, *8*, 115–123.
- (8) Baehr, A. L.; Stackelberg, P. E.; Baker, R. L. Evaluation of the atmosphere as a source of volatile organic compounds in shallow groundwater. *Water Resour. Res.* **1999**, *35*, 127–136.
- (9) Falta, R. W.; Javandel, I.; Pruess, K.; Witherspoon, P. A. Density driven flow of gas in the unsaturated zone due to the evaporation of volatile organic components. *Water Resour. Res.* **1989**, *25*, 2159–2169.
- (10) Costanza-Robinson, M. S.; Brusseau, M. L. Gas phase advection and dispersion in unsaturated porous media. *Water Resour. Res.* **2002**, *38*, 71–79.
- (11) Ostendorf, D. W.; Campbell, D. H. Biodegradation of hydrocarbon vapors in the unsaturated zone. *Water Resour. Res.* **1991**, *27*, 453–462.
- (12) Hers, I.; Atwater, J.; Li, L.; Zapf-Gilje, R. Evaluation of vadose zone biodegradation of BTX vapours. *J. Contam. Hydrol.* **2000**, *46*, 233–264.
- (13) Dakhel, N.; Pasteris, G.; Werner, D.; Höhener, P. Small-volume releases of gasoline in the vadose zone: Impact of the additives MTBE and ethanol on groundwater quality. *Environ. Sci. Technol.* **2003**, *37*, 2127–2133.
- (14) Kaufmann, K.; Christophersen, M.; Buttler, A.; Harms, H.; Höhener, P. Microbial community response to petroleum hydrocarbon contamination in the unsaturated zone at the experimental field site Værløse, Denmark. *FEMS Microbiol. Ecol.* **2004**, *48*, 387–399.
- (15) Pasteris, G.; Werner, D.; Kaufmann, K.; Höhener, P. Vapor phase transport and biodegradation of volatile fuel compounds in the unsaturated zone: a large scale lysimeter experiment. *Environ. Sci. Technol.* **2002**, *36*, 30–39.
- (16) Lahvis, M. A.; Baehr, A. L. Estimation of rates of aerobic biodegradation by simulation of gas transport in the unsaturated zone. *Water Resour. Res.* **1996**, *32*, 2232–2249.
- (17) El-Farhan, Y. H.; Scow, K. M.; de Jonge, L. W.; Rolston, D. E.; Moldrup, P. Coupling transport and biodegradation of toluene and trichloroethylene in unsaturated soils. *Water Resour. Res.* **1998**, *34*, 437–445.
- (18) Karapanagioti, H. K.; Gaganis, P.; Burganos, V. N. Modeling attenuation of volatile organic mixtures in the unsaturated zone: codes and usage. *Environ. Modell. Softw.* **2003**, *18*, 329–337.
- (19) Karapanagioti, H. K.; Gaganis, P.; Burganos, V. N.; Höhener, P. Reactive transport of volatile organic compound mixtures in the unsaturated zone: modelling and tuning with lysimeter data. *Environ. Modell. Software* **2004**, *19*, 435–450.
- (20) Gaganis, P.; Kjeldsen, P.; Burganos, V. N. Modeling natural attenuation of multicomponent fuel mixtures in the vadose zone: use of field data and evaluation of biodegradation effects. *Vadose Zone J.* **2004**, *3*, 1262–1275.
- (21) Suchomel, K. H.; Kremer, D. K.; Long, A. Production and transport of carbon dioxide in a contaminated vadose zone: A stable and radioactive carbon isotope study. *Environ. Sci. Technol.* **1990**, *24*, 1824–1831.
- (22) Aggarwal, P. K.; Hinchee, R. E. Monitoring in situ biodegradation of hydrocarbons by using stable carbon isotopes. *Environ. Sci. Technol.* **1991**, *25*, 1178–1180.
- (23) Jackson, A.; Pardue, J. Quantifying the mineralization of contaminants using stable carbon isotope ratios. *Org. Geochem.* **1999**, *30*, 787–792.
- (24) Conrad, M. E.; DePaolo, D. J. Carbon isotopic evidence for biodegradation of organic contaminants in the shallow vadose zone of the radioactive waste management complex. *Vadose Zone J.* **2004**, *3*, 143–153.
- (25) Kirtland, B. C.; Aelion, C. M.; Stone, P. A. Assessing in situ mineralization of recalcitrant organic compounds in vadose zone sediments using delta<sup>13</sup>C and <sup>14</sup>C measurements. *J. Contam. Hydrol.* **2005**, *76*, 1–18.
- (26) Kirtland, B. C.; Aelion, C. M.; Stone, P. A.; Hunkeler, D. Isotopic and geochemical assessment of biodegradation of chlorinated hydrocarbons. *Environ. Sci. Technol.* **2003**, *37*, 4205–4212.
- (27) Stehmeier, L. G.; Francis, M. M.; Jack, T. R.; Diegor, E.; Winsor, L.; Abrajano, T. A. J. Field and in vitro evidence for in-situ bioremediation using compound-specific <sup>13</sup>C/<sup>12</sup>C ratio monitoring. *Org. Geochem.* **1999**, *30*, 821–833.
- (28) Cerling, T. E.; Solomon, D. K.; Quade, J.; Bowman, J. R. On the isotopic composition of carbon in soil carbon dioxide. *Geochim. Cosmochim. Acta* **1991**, *55*, 3403–3405.
- (29) Reitsem, R. H.; Kaltenback, A. J.; Lindberg, F. A. Source and migration of light hydrocarbons indicated by carbon isotopic ratios. *Bull. Am. Assoc. Pet. Geol.* **1981**, *65*, 1536–1542.
- (30) Galimov, E. M. A<sup>13</sup>C isotope enrichment effect in methane carbon in the course of its infiltration through rocks. *Geochem. Int.* **1967**, *4*, 1180–1181.
- (31) Pernaton, E.; Prinzhofer, A.; Schneider, F. Reconsideration of methane signature as a criterion for the genesis of natural gas: influence of migration on isotopic signature. *Rev. IFP* **1996**, *51*, 635–651.
- (32) Zhang, T.; Krooss, B. M. Experimental investigation on the carbon isotope fractionation of methane during gas migration by diffusion through sedimentary rocks at elevated temperature and pressure. *Geochim. Cosmochim. Acta* **2001**, *65*, 2723–2742.
- (33) Broholm, M. M.; Christophersen, M.; Maier, U.; Stenby, E. H.; Höhener, P.; Kjeldsen, P. Compositional Evolution of the Emplaced Fuel Source in the Vadose Zone Field Experiment at Airbase Værløse, Denmark. *Environ. Sci. Technol.* **2005**, *39*, 8251–8263.
- (34) Hunkeler, D.; Aravena, R. Determination of stable carbon isotope ratios of chlorinated methanes, ethanes and ethenes in aqueous samples. *Environ. Sci. Technol.* **2000**, *34*, 2839–2844.
- (35) Clark, I. D.; Fritz, P. *Environmental isotopes in hydrogeology*; Lewis Publishers: Boca Raton, FL, 1997.
- (36) Katyal, A. K.; Kaluarachchi, J. J.; Parker, J. C.; Cho, J. S.; Swaby, L. G. *MOFAT: A two-dimensional finite element program for multiphase flow and multicomponent transport*, EPA/600/2-91/020; U.S. EPA: Washington, DC, 1991.
- (37) Harrington, R. R.; Poulson, S. R.; Drever, J. I.; Colberg, P. J. S.; Kelly, E. F. Carbon isotope systematics of monoaromatic hydrocarbons: vaporization and adsorption experiments. *Org. Geochem.* **1999**, *30*, 765–775.
- (38) Gaganis, P.; Karapanagioti, H. K.; Burganos, V. N. Modelling multicomponent NAPL transport in the unsaturated zone with the constituent averaging technique. *Adv. Water Resour.* **2002**, *25*, 723–732.
- (39) Craig, H. The geochemistry of stable carbon isotopes. *Geochim. Cosmochim. Acta* **1953**, *3*, 53–92.
- (40) Jost, W. *Diffusion in Solids, Liquids and Gases*; Academic Press: New York, 1960; Vol. 3.
- (41) Stahl, W.; Faber, E.; Carey, B. D.; Kirksey, D. L. Near-surface evidence of migration of natural gas from deep reservoirs and source rocks. *Bull. Am. Assoc. Pet. Geol.* **1981**, *65*, 1543–1550.
- (42) Bouchard, D. Use of stable isotope analysis to assess biodegradation of volatile organic compounds in the unsaturated subsurface. Ph.D. Thesis, Université de Neuchâtel, Neuchâtel, 2007; p 127.
- (43) Bouchard, D.; Hunkeler, D.; Höhener, P. Carbon isotope fractionation during aerobic biodegradation of *n*-alkanes and aromatic compounds under unsaturated soil conditions. *Org. Geochem.* In press.
- (44) Bouchard, D.; Hunkeler, D.; Höhener, P.; Aravena, R.; Broholm, M.; Kjeldsen, P. Use of stable isotope analysis to assess biodegradation of petroleum hydrocarbons in the unsaturated zone. Laboratory studies, field studies, and mathematical simulations. In *Reactive Transport in Soil and Groundwater: Processes and Models*; Nützmänn, G. V. P., Aagaard, P., Ed.; Springer-Verlag: Berlin, 2005; pp 17–38.